Biological impacts of Ce nanoparticles with different surface coatings as revealed by RNA-Seq in *Chlamydomonas reinhardtii*

Elise Morel[a], Ibrahim Jreije[a], Valerie Tetreault[a], Charles Hauser[b], William Zerges[c], Kevin J. Wilkinson[a,Ψ]

[a]Biophysical Environmental Chemistry Group, University of Montreal, P.O. Box 6128, Succ. Centre-Ville, H3C 3J7, Montreal, QC, Canada

[b]Biological Sciences, St. Edward's University, 3001 S Congress Ave, 78704, Austin, TX, USA

[c]Dept. of Biology, Concordia University, 7141 Sherbrooke W., H4B 1R6, Montreal, QC, Canada

[Ψ] kj.wilkinson@umontreal.ca; ORCID: 0000-0002-7182-3624

Accepted for publication : *Nanoimpact*, 2020, 19: 100228; DOI: 10.1016/j.impact.2020.100228

ABSTRACT

In order to better understand the risks of engineered nanoparticles (ENPs), it is necessary to determine their fate and biological effects under realistic exposure scenarios (e.g. low ENP concentrations). RNA-Seq was deployed to characterize the relative biological impacts of three small Ce ENPs (i.e. nominal size <20 nm, 70 µg L^{-1} Ce), with different coating properties (i.e. uncoated, citrate or poly-acrylic acid coated), towards a unicellular freshwater microalga, *Chlamydomonas reinhardtii*. After 2 h exposition at pH 7.0, distinct differences in transcriptomic effects were observed when comparing ionic Ce and Ce ENPs. Notably, Ce ENPs specifically modulated mRNA levels of genes related to the ubiquitin-proteasome system and to flagella structure. Compared to control conditions, transcriptomic effects induced by the citrate coated Ce ENPs were rather limited, as only 23 genes were differentially expressed by this treatment ($Log_2FC > |1.0|$, $p_{adj} < 0.001$); compared to uncoated Ce ENPs (688); polyacrylic coated Ce ENPs (315) or a similar concentration of ionic Ce (138). Somewhat surprisingly, similar changes in the algal transcriptomes were observed for treatments with poly-acrylic acid coated Ce ENPs (mainly Ce(III), little dissolution) and uncoated Ce ENPs (mainly Ce(IV) atoms, largely agglomerated) ($Log_2FC > |1.0|$, $p_{adj} < 0.001$). For the moderate exposure concentrations examined here, toxicity appeared to be minimal for both ionic Ce and Ce ENPs. Nonetheless, an important number of genes could not be assigned to a biological pathway. The study gives important insights with respect to the role of particle surface coatings on biological effects, the mechanisms of interaction of Ce ENP with a green alga, in addition to identifying several useful transcriptomic biomarkers of Ce ENP exposure.

GRAPHICAL ABSTRACT

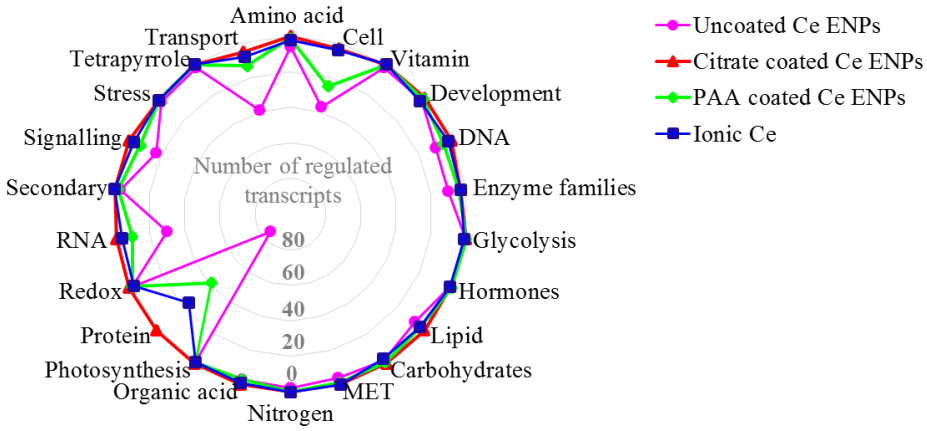

KEYWORDS

Cerium engineered nanoparticles, coatings, transcriptomic analysis, bioavailability, microalgae.

ABBREVIATIONS

ENPs, engineered nanoparticles; PAA, polyacrylic acid; SP-ICP-MS, single particle inductively coupled plasma mass spectrometry; RNA-Seq, RNA sequencing, DEGs, differentially expressed genes.

1. Introduction

Of the rare earth elements, cerium (Ce) is one of the most used.[1] Its optical and catalytic properties make it an important element in numerous applications, including high technology and green technology industries.[2,3] For example, Ce is incorporated as salts into solid oxide fuel cells[4] or, as engineered nanoparticles (ENPs), into diesel additives.[5] While these technologies enhance energy efficiency, they also can lead to widespread environmental contamination of Ce.[6-8] Novel applications of Ce ENPs in biomedicine,[9] agriculture[10] and water depollution[11] are also expected to increase environmental concentrations.

Contradictory results have been observed in the literature with respect to the biological effects of Ce ENPs towards aquatic micro-organisms. Indeed, it is still not clear if the biological effects of Ce ENPs are due to the nanoparticles themselves or to their dissolution products. For example, several authors have shown that the dissolved Ce that co-occurred in nanoparticle suspensions had negligible effects with respect to the Ce ENPs, even for concentrations of dissolved Ce up to 5 µg L^{-1}.[12,13,14] In contrast, using similar concentrations of dissolved Ce, Röhder *et al*. related biological responses in phytoplankton to the dissolved Ce rather than the Ce ENPs.[15] Part of the discrepancy between these contradictory results may be due to differences in the intrinsic properties of the ENPs that were tested (e.g. size, shape, coatings[16]) and the experimental conditions that were deployed (e.g. pH, ligand concentrations). Specifically, coatings such as polyacrylic acid[12] or polyvidone[13] can provide greater Ce ENP colloidal stability (prevent ENP agglomeration or dissolution) or act as a protective barrier, preventing direct contact of the particle core with the biological membrane. Citrate has been shown to stabilize Ce ENPs for up to 6

weeks[19] and mitigate bacteria-mediated reduction of Ce ENPs.[20] The aqueous-ENP interface is thus a major critical factor influencing the biological impact of Ce ENPs, resulting from the Ce(III)/Ce(IV) ratio,[21,22] the surface charge,[23,17] the specific surface area[14], the nature of the surface coating,[24] and ENP size (especially with respect to the diameters of pores in the cell wall, i.e. 15-20 nm).[17,18]

There is still no consensus on the overall impact of ENP surface coatings[25] on the biological effects of Ce ENP to microalgae. For example, median effective concentrations (72 h EC50s) for the growth inhibition of microalgae have ranged from 0.024 mg L^{-1} to 29.6 mg L^{-1}: polyacrylate coated Ce ENPs (4-10 nm, 0.024 mg L^{-1}),[12] citrate stabilized Ce ENPs (10 nm, 5.6 mg L^{-1})[26] and uncoated Ce ENPs (10 nm and <25 nm, 2.4–29.6 mg L^{-1};[27] 10-20 nm, 10.3 mg L^{-1} [28]); while no adverse effects on growth were measured for polyvidone coated Ce ENPs (4-7 nm, >80 mg L^{-1}).[13] Moreover, toxic effects are often reported for exposures to mg L^{-1} of Ce ENPs, whereas, generally only ng L^{-1} concentrations are thought to be found in natural waters.[29] Recent studies using transcriptome profiling by RNA sequencing (RNA-Seq) have shown patterns of gene expression that correlate with the physicochemical properties of ENPs.[30,31] For Ce ENPs, gene expression has been notably used to distinguish the effects of particle sizes (micro or nano)[32] or the degree of degradation of a citrate coating.[24] Nonetheless, while Taylor *et al.* observed significant differential gene expression following a 3-d exposure of *C. reinhardtii* to 10 mg L^{-1} of polyvidone coated Ce ENPs, no effects were observed at more environmentally relevant concentrations of 0.144 µg L^{-1}.[13] Clearly, further systematic studies on the biological effects of Ce ENPs with different coating properties are required, especially at environmentally relevant Ce ENP concentrations.

In this study, RNA-Seq was used to compare the effects of ionic Ce and small Ce ENPs (<20 nm) with different coatings: uncoated, stabilized by citrate, and coated by poly-acrylic acid., on the transcriptome of *C. reinhardtii* exposed to moderate Ce ENP concentrations (70 µg L^{-1} Ce). Multi-method characterization experiments, including single particle inductively coupled plasma mass spectrometry (SP-ICP-MS), were performed to determine the physicochemical stability of the Ce ENPs.

2. Materials and methods

2.1. Materials

All experiments were performed in polymerware (polypropylene or polycarbonate) or Teflon, which was first soaked in 2% v/v HNO_3 for 24 hours, rinsed 7x with Milli-Q water (total organic carbon < 2×10^{-3} g L^{-1}; resistivity > 18 MΩ cm) and dried under laminar flow conditions (Heraeus). Most reagents were purchased from Fisher Scientific (molecular biology grade), except acetic acid (analytical grade, Fisher Scientific), chloroform (99,8%, Acros organics) and nuclease-free water (QIAGEN). Other chemicals included: K_2HPO_4 and KH_2PO_4 (ACS reagent grade, Fisher Chemical), Tris (Tris-(hydroxymethyl)-aminomethane, BDH USP/EPgrade, VWR), EDTA disodium salt (Bioultra grade, Sigma-Aldrich), Isotone (VWR), HNO_3 (67–70%; BDH Aristar Ultra, VWR), H_2O_2 (30%, BDH Aristar Ultra, VWR), NaOH (Acros Organics), NaMES (2-(N-morpholino)ethanesulfonic sodium salt, Acros Organics), NaHEPES (4-(2-hydroxyethyl)-1-piperazineethanesulfonic sodium salt, Acros Organics).

2.2. Preparation and characterization of the nanoparticles

2.2.1. Nanoparticles

$Ce(NO_3)_3$ (**ionic Ce**) was purchased from Inorganic Ventures (1.0 g L^{-1}; ICP-MS standard). **Uncoated Ce ENPs** (nominally 15 - 30 nm) were purchased from Nanostructured & Amorphous Materials as a powder (1406RE). Triammonium **citrate stabilized Ce ENPs** (nominally 10 nm) were obtained from Byk (Nanobyk®-3810). The measured Ce concentration of the stock solution was 187.6 ± 2.7 g L^{-1} Ce ENPs. Sodium **polyacrylic acid coated Ce ENPs** (PAA coated Ce ENPs) (nominally 1-10 nm) were obtained from Sciventions as an aqueous suspension (1.5 g L^{-1} Ce ENPs) and as a powder. Intermediate 1 g L^{-1} suspensions of all ENPs were prepared in polypropylene tubes that were covered with aluminum foil and stored at 4°C. Before use, they were manually shaken and sonicated (sonication bath, 135W, 30 min.), prior to their dilution in the experimental media, where they were equilibrated for 24 h with orbital shaking (100 rpm) at room temperature.

2.2.2. Concentrations

Ce concentrations were determined by adding 400 µL of HNO_3 (67–70%) and 300 µL of H_2O_2 (30%) to 1 mL of sample and then heating the mixture at 80° C for 5 h (DigiPREP, SCP science). Samples were analyzed by inductively coupled plasma mass spectrometry (**ICP-MS**, PerkinElmer; NexION 300X). A Ce calibration curve was run every 20 samples while blanks and quality control standards were run every 10 samples. Indium was used as an internal standard to correct for instrumental drift.

2.2.3. TEM and EDS

ENP size was characterized by transmission electron microscopy (**TEM**) and energy-dispersive x-ray spectroscopy (**EDS**) on a JEOL (model JEM-2100F) microscope. Three drops of a 1.0×10^{-2} g L^{-1} ENP suspension in Milli-Q water were deposited and dried on Cu holey electron microscopy grids (200 mesh; Electron Microscopy Sciences) under laminar flow. Particle diameters were determined using ImageJ ($n\geq50$).[33,34]

2.2.4. SP-ICP-MS

A sector field ICP-MS (Nu Attom, Nu instruments, UK) in single particle mode (**SP-ICP-MS**) was used to quantify the particle size distribution and dissolution of the ENP suspensions at 70.1 µg L^{-1} Ce. Samples were diluted immediately prior to analysis in order to have 1000 – 2000 peaks per measurement time (50 s), which is optimal to avoid concurrent ionization of more than one ENP, while providing statistically significant particle numbers (**Figure A.1**). A dwell time of 50 µs, a sample flow rate of 200-250 µL.min^{-1}, a concentric glass nebulizer (internal diameter: 1.5 mm) and a quartz cyclonic spray chamber cooled to 4°C were employed. The isotope ^{140}Ce was monitored and calibration was performed using ionic standards (Inorganic Ventures, CGCE-1) in the range of 0.05 to 2.0 µg L^{-1}. A transport efficiency of 3-5 % was determined from a suspension of 30 nm ultra-uniform gold nanoparticles (Nanocomposix, AUXU30-1M, 20.0×10^{-9} g L^{-1}).[35] It was validated using a suspension of 20 nm silver nanoparticles (NanoXact, ECP1691, 20.0×10^{-9} g L^{-1}) and by frequent analysis of an ionic In standard to document sensitivity variations. Data were processed using NuQuant software (version

2.2), details on single particle ICP-MS and the data processing can be found in **Supplementary information** and elsewhere.[35-37]

2.2.5. Centrifugal ultrafiltration

ENP dissolution in the algal exposure media was also monitored using centrifugal ultrafiltration units (Amicon ultra-4, 3 kDa molar mass cutoff). Four mL samples were centrifuged for 20 min at 3700×g at 20 °C. In order to minimize adsorptive losses to the ultrafiltration membrane, the filtrate was collected after the third centrifugation cycle and analyzed by ICP-MS (**Figure A.2**). Mass balances were determined from Ce concentrations: (i) in the filtrate; (ii) in the solution remaining above the filter; and (iii) in an acid (69% v/v HNO_3) extraction of the filter. For blanks, Ce was below detection limits of ICP-MS (~40 ng L^{-1}).

2.2.6. Electrophoretic mobility and DLS

Electrophoretic Mobility (**EPM**) and Dynamic Light Scattering (**DLS**) measurements were performed at 20°C in the PEEK flow cell of the Möbiuζ (Wyatt Instruments, 532 nm laser and 168.7° scattering angle). Hydrodynamic diameters and EPM were obtained for 40-50 mg L^{-1} of Ce ENPs in pH buffered exposure media (NaMES: pH 5.0-6.0; NaHEPES: pH 6.5-8.5 containing 10.0 µM of $Ca(NO_3)_2$). A regularization algorithm (7.3.1.15 DynamicSoftware) was used to analyze the DLS autocorrelation function. Diffusion coefficients were converted to hydrodynamic diameters using the Stokes−Einstein equation. The analytical performance of the instrument was systematically verified using a NIST polystyrene standard (Bangs Laboratories, NT02N) with a known diameter of 42 nm that was diluted to 20% (v/v) in Milli-Q water. Experiments were

duplicated using freshly prepared samples that were analyzed on separate days. Each individual replicate was divided into two aliquots, which were each analyzed 4x.

2.2.7. Analytical ultracentrifugation

Analytical ultracentrifugation (**AUC**, ProteoLab XLI analytical ultracentrifuge, Beckman XLI)) using interference detection, was performed using 400 μL of the same suspensions that were used for DLS. Sedimentation profiles (900 scans) were generated by ultracentrifuging the samples at 18,144×g for uncoated Ce ENPs, 26,127×g for citrate stabilized Ce ENPs and 72,576×g for PAA coated Ce ENPs. The sedimentation coefficient distribution was determined using SEDFIT (v. 14.1). By assuming a particle density of ρ=7.13 g cm^{-3} for uncoated and citrate stabilized Ce ENPs (https://www.nanoamor.com/msds/msds_CeO_2_1406RE.pdf) and ρ=2.00 g cm^{-3} for the PAA coated Ce ENPs (ρ=1.09 g cm^{-3} for the organic polymer[38] (85 dry wt.%) and ρ=7.13 g cm^{-3} for CeO_2 (15 dry wt.%)), particle size distributions could be determined based on the Stokes−Einstein equation. Further theoretical and methodological considerations are provided in Diaz *et al.*, 2015.[38]

2.2.8. X-ray photoelectron spectroscopy

Ce(III)/Ce(IV) ratios were analyzed to a depth of ~5 nm by x-ray photoelectron spectroscopy (**XPS**) on the ENPs powders. XPS spectra were recorded on a VG ESCALAB 3MKII spectrometer using Mg Kα radiation ($h\nu$= 1253.6 eV). Photoelectrons were detected at 90° with respect to the sample surface. High resolution XPS spectra were obtained for C1s (280-290 eV), O1s (525-535 eV), Ce3d (875-920 eV). Peak fitting (Lorentzian-Gaussian curves) was performed with Avantage software (Thermo Scientific) after a

background subtraction (Shirley function). The energies 881.6, 885.1, 899.2 and 903.5 eV were used as component peaks for Ce(III) and 882.6, 888.4, 898.2, 901.1, 906.7 and 916.5 eV as component peaks for Ce(IV).

2.3. Culture conditions

C. reinhardtii (Wild type CC-125 (aka 137c) from the *Chlamydomonas* resource center) was inoculated from agar-solidified (1.5% wt/v) Tris-acetate-phosphate (TAP)[39] medium into 75 mL of a 4×diluted TAP medium.[40] This green microalga is ubiquitous to fresh waters and is often used for water quality monitoring and studies examining the toxicology of pollutants in natural waters. The culture was grown at 20°C under conditions of 12 h light/12 h dark (60 mmol s^{-1} m^{-2}), with orbital shaking (100 rpm). Once the culture reached its mid-exponential growth phase (1-5×10^6 cells mL^{-1}; ~3 d), it was used to inoculate 400 mL of 4×diluted TAP. This culture was also grown until a mid-exponential phase (~2 d) and then centrifuged at 2000×g for 3 min to pellet the cells. The cell pellet was resuspended in 10 mM NaHEPES (pH 7.0), containing no metal. This wash procedure was repeated twice in order to prepare a cell concentrate that was added to the exposure solutions (below). Cell concentrations and cell surface areas were measured using a Multisizer 3 particle counter (50 mm aperture; Beckman Coulter).

2.4. Exposure conditions

Approximately 6.5 x 10^4 cells mL^{-1} were exposed for 2 h to 0.5 µM of Ce (70.1 µg L^{-1} Ce and 86.1 µg L^{-1} for Ce ENPs) in 10.0 mM NaHEPES at pH 7.0 containing also 10.0 µM $Ca(NO_3)_2$.[41] Control treatments were also conducted in similar exposure medium but without the addition of any Ce forms. This simplified experimental medium was used so

that the chemical speciation of Ce could be precisely controlled. For example, Ce precipitates in the presence of phosphate, which is routinely found in algal growth media. In order to evaluate adsorptive losses and potential contamination, metal concentrations in the media were measured at the start and end of each experiment. Short term exposures and low cellular densities of the microalgae were used in order to limit variations in Ce concentrations and speciation during the exposure (**Figure A.3**). Microalgae can modify trace metal exposure concentrations by adsorption and/or biouptake and they produce exudates that may modify the speciation of Ce.[41, 42] It was previously shown in our group that 2h exposures of *C. reinhardtii* to trace metals[43] or nanoparticles[44] was sufficient to induce significant changes at the transcriptional level, while minimizing changes in solution chemistry and cell numbers. Following the 2h exposure, cells were pelleted by centrifugation from 300 mL of the exposure solution (2000×g, 2 min., 4°C). Cell pellets were resuspended in 1 mL nuclease-free water before being transferred into 1.5 mL microtubes where the cells were again pelleted by centrifugation. Cell pellets were frozen on dry ice for 10 minutes and stored at −80 °C.

2.5. RNA-Seq analysis

2.5.1. RNA preparation

Cell pellets were thawed and then immediately resuspended in freshly prepared lysis buffer (0.3 M NaCl, 5.0 mM EDTA, 50 mM Tris-HCl (pH 8.0), 2.0% SDS, 3.3 U mL^{-1} proteinase K) where they were incubated at 37 °C for 15 min. Total RNA was isolated by extracting the sample 3x with phenol:chloroform:isoamyl alcohol (25:24:1, pH 6.8) followed by 1x with chloroform:isoamyl alcohol (24:1). At each step, samples were

centrifuged (12000xg, 10 min., 4° C) and supernatants were transferred into new tubes. Total RNA was precipitated from the final aqueous phase by isopropanol, then washed with 75% ethanol. After a final centrifugation, the pellet was resuspended in 20-30 µL of nuclease-free water. An aliquot (3 µL) was analyzed by automated electrophoresis for RNA quality (RIN number > 7, 1.8 < ratio 260/280 < 2.1, ratio 260/230>1.8; Bioanalyzer, Agilent) and spectroscopy (OD260) to determine the concentration of RNA (Nanodrop).

2.5.2. cDNA library construction and high-throughput sequencing

mRNA selection, library preparation (NEB/KAPA mRNA stranded library preparation) and Illumina sequencing were carried out at the Genome Quebec facilities (www.gqinnovationcenter.com). Two lanes on a HiSeq (v4) were used for the paired-end sequencing (2 × 125 base pairs) of 16 samples (3 replicates for each Ce treatment: ionic Ce; uncoated Ce ENPs; citrate stabilized Ce ENPs; PAA coated Ce ENPs) and 4 replicates for controls). Replicates (biological) were each from independent cultures.

2.5.3. Sequence analysis, differential expression and functional annotation

For each sample, *ca.* 64 million reads were obtained by Illumina sequencing. Read quality was explored with FastQC[45]. Filtering quality and adapter trimming were conducted with Trim Galore!.[46] Only paired reads obtained after the cleaning step (phred >20, length > 21 bp) were conserved. Reads were aligned to the *C. reinhardtii* genome v5.3 assembly using TopHat2 with standard presets except that intron size was between 30 and 28000 bbp.[47] Approximately 60 million reads were mapped for each sample (around 93% of $(64.2 \pm 2.2)\times10^6$ reads; **Table A.1**) with multiple-read alignments accounting for 5.8 ± 0.2% of the total mapped reads in each sample. GeneBody coverage python script

(RSeQC) was used to calculate the number of reads for each nucleotide position and to generate a plot illustrating the coverage profile along the gene (**Figure A.7**).[48] The number of reads per gene was determined using the Python package HTSeq.[49] Differentially expressed transcripts were identified using DESeq2 for $\log_2$ fold change (Log_2FC) values exceeding |1| and false discovery rates (p_{adj}) < 0.001.[50] Gene annotations were retrieved from MapMan ontology.[51,52] The JGI Comparative Plant Genomics Portal was also used to explore the function of gene sets of interest, such as the "unclassified" gene list obtained from MapMan (**Supplementary Data 7**).[53] The Wilcoxon rank-sum test was used to identify enriched metabolic pathways. The Algal Functional Annotation Tool was used to convert gene and transcript ID, when necessary.[54]

3. Results and discussion

3.1. ENP Characterization

Although the three ENPs were initially thought to be very similar (based upon manufacturer's indications), several important differences (e.g. state of agglomeration, proportion of Ce(III)) were noted following characterization experiments. The key results of the ENP characterization are summarized in **Table 1** with numerous additional details provided in the SI (**Figures A.4, A.5 and A.6**).

By combining data from the different techniques (**Table 1**), it was possible to conclude that under the conditions of the algal exposures (70.1 µg L^{-1} Ce in NaHEPES at pH 7.0), the Ce ENPs had a mean primary particle size of <10 nm with a negative surface potential (EPMs of -0.8 ± 0.5 µm.cm/s.V for the uncoated Ce ENPs; -1.4 ± 0.3 µm.cm/s.V

for the citrate coated Ce ENPs; -1.6 ± 0.2 µm.cm/s.V for PAA coated Ce ENPs). Of the three ENP types, the uncoated Ce ENPs were most subject to agglomeration. Nonetheless, SP-ICP-MS results indicated some agglomeration of the citrate stabilized Ce ENPs at low particle concentrations, potentially due to a desorption of the citrate from the particle surface following dilution.[55] Consistent with their propensity for agglomeration, the greatest losses of Ce from the exposure medium were observed for the uncoated and citrate stabilized ENPs, where only about half of the starting Ce was recovered: ionic Ce (60.7 ± 3.9 µg L^{-1} Ce), uncoated Ce ENPs (39.3 ± 10.0 µg L^{-1} Ce), citrate stabilized Ce ENPs (33.2 ± 5.6 µg L^{-1} Ce), and PAA coated Ce ENPs (70.7 ± 2.2 µg L^{-1} Ce) (**Figure A.3, Table 1)**. These losses were likely caused by sedimentation of the largest agglomerates. Nonetheless, during the following 2h exposure of microalgae, measured Ce concentrations remained reasonably stable **(Figure A.3)**. The PAA coated Ce ENPs did not appear to be 'classical' Ce(IV) ENPs: in contrast to the manufacturer's data, XPS indicated that Ce was entirely Ce(III), either complexed by the PAA coating or precipitated as Ce_2O_3. This discrepancy could be explained by an expected structural transformation from CeO_2 to Ce_2O_3 that is observed for small (< 20 nm) Ce ENPs.[56,57] Nonetheless, an underestimation of the core Ce(IV) cannot be excluded for these ENPs as Ce reduction may be amplified by XPS analyses under vacuum and/or X-ray radiation.[58] For all exposure media containing Ce ENPs, only negligible dissolved Ce was detected. Furthermore, in the solutions of ionic Ce, up to 20% of the Ce could be classified as incidental nanoparticles (**Table 1**), corresponding to cerium oxides (CeO_2), hydroxides ($Ce(OH)_4$), or other metastable, pH sensitive species[59,60] such as cerium oxides or carbonates.

Table 1. ENP mean diameters, polydispersity index (PDI), % of mass detected as ENPs and recovery obtained for TEM, AUC, DLS, SP-ICP-MS or analysis by ultrafiltration (3 kDa membrane) for uncoated, citrate stabilized and PAA coated Ce ENPs in NaHEPES at pH 7.0.

$[Ce]_T$ (µg L^{-1})	Technique	Type of diameter	Mean size distribution (nm)	PDI	% of ENPs detected	Recovery (%)
Ionic Ce						
0.0039 ± 0.0005	SP-ICP-MS	d_p	8.4 ± 0.3	0.16 ± 0.07	35.7 ± 27.7	41.8 ± 2.1
66.6 ± 9.5	Ultrafiltration	-	-	-	21.3 ± 11.3	106.5 ± 2.3
Uncoated (Nanostructured & Amorphous Materials)						
10,380	TEM	d_p	9.7 ± 2.8	-	-	-
50,000 ± 2,000	AUC	d_h	8.0 ± 0.1	0.29 ± 0.04	90.5 ± 3.6	-
50,000 ± 2,000	DLS	d_h	6692 ± 2026	0.51 ± 0.23	100 ± 0.0	-
0.050 ± 0.014	SP-ICPMS	d_p	19.7 ± 1.2	0.95 ± 0.10	98.5 ± 2.1	9.2 ± 0.3
50.5 ± 9.7	Ultrafiltration	-	-	-	99.9 ± 0.0	101.1 ± 3.6
Citrate stabilized (Byk)						
9,780	TEM	d_p	4.4 ± 0.9	-	-	-
42,400 ± 300	AUC	d_h	4.1 ± 0.1	0.02 ± 0.01	96.6 ± 3.0	-
42,400 ± 300	DLS	d_h	6.2 ± 0.3	0.13 ± 0.03	99.6 ± 0.3	-
0.022 ± 0.010	SP-ICP-MS	d_p	22.9 ± 2.4	0.34 ± 0.08	99.0 ± 0.6	57.6 ± 9.5
55 ± 25	Ultrafiltration	-	-	-	99.8 ± 0.2	82.5 ± 0.7
PAA coated (Sciventions)						
9,980	TEM	d_p	3.0 ± 0.8	-	-	-
47,400 ± 500	AUC	d_h	3.1 ± 0.3	0.39 ± 0.05	90.2 ± 2.8	-
47,400 ± 500	DLS	d_h	5.9 ± 2.9	0.64 ± 0.28	99.6 ± 0.4	-
0.0049 ± 0.0014	SP-ICP-MS	d_p	9.9 ± 2.5	0.32 ± 0.29	9.3 ± 2.4	44.6 ± 8.6
70.4 ± 2.9	Ultrafiltration	-	-	-	99.5 ± 0.9	99.7 ± 8.7

Errors correspond to standard deviations obtained for 2 to 4 replicates while PDI gives an indication of the overall particle size distribution. d_h: hydrodynamic diameter; d_p: physical diameter.

3.2. Overview of the RNA-Seq data

Of the 19,526 predicted transcripts in *C. reinhardtii*,[61] 16,808 (86%) were detected, indicating that the RNA-Seq data was high quality and unbiased (**Supplementary Data 1**). Eight hundred and forty-eight (848) genes showed at least a 2-fold change with respect to

their control values in one or more of the treatments **(Figure 1, Supplementary Data 2)**. When those DEGs were analyzed by principal component analysis (PCA), data were grouped around the Ce ENPs (associated with PC1, 54% of variance) and ionic Ce (associated with PC2, 23% of variance) (**Figure A.8.B**). Moreover, the uncoated Ce ENPs and the PAA coated Ce ENPs were distinctly grouped from the citrate stabilized Ce ENPs in the variable space of the PCA plot (**Figure A.8.B**). Comparisons of the profiles of DEGs elicited by each of the Ce ENPs, i.e. their "transcriptomic signatures", suggest that bioavailability was highest for the uncoated Ce ENPs, intermediate for the PAA coated Ce ENPs, and lowest for the citrate stabilized Ce ENPs. In the sections that follow, we first discuss the results that nano-specific effects were observed (**Section 3.3**) and then secondly, the nature of the differences that were observed among the different Ce ENP surface coatings (**Section 3.4**).

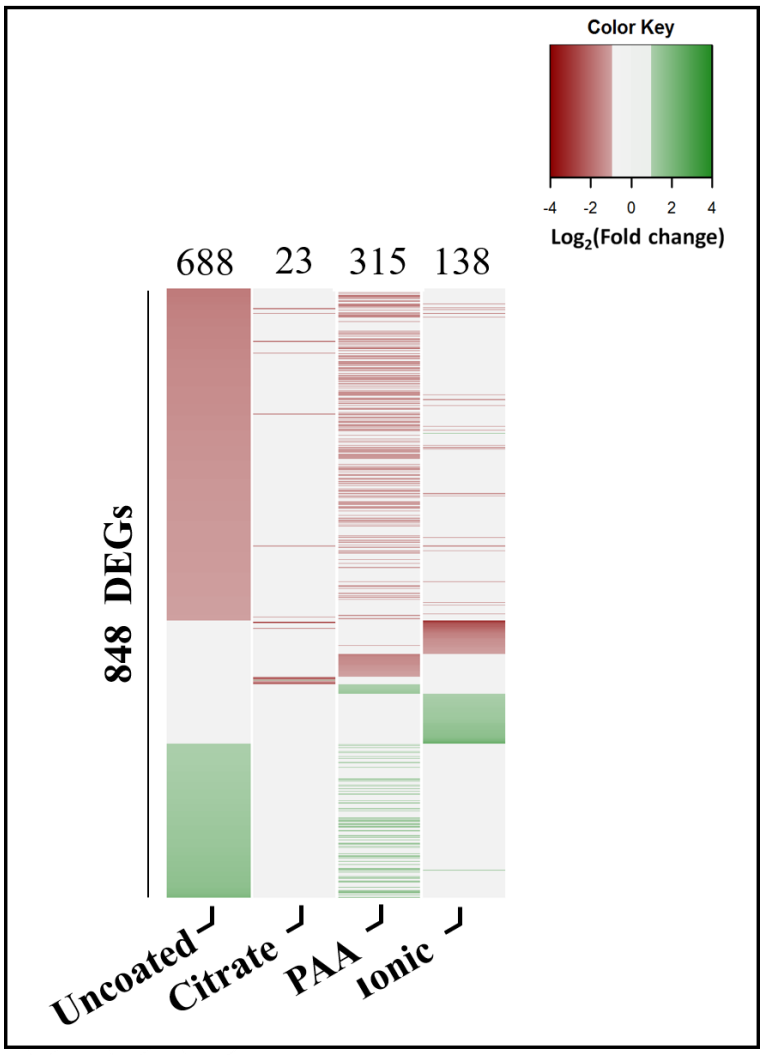

Figure 1. – Differentially expressed genes with respect to the control ($Log_2FC > |1|$, $p_{adj} < 0.001$), following a 2 h exposure of *C. reinhardtii* to uncoated Ce ENPs (39.3 ± 10.0 µg L^{-1}), citrate stabilized Ce ENPs (33.2 ± 5.6 µg L^{-1}), PAA coated Ce ENPs (70.7 ± 2.2 µg L^{-1}), and ionic Ce (60.7 ± 3.9 µg L^{-1}). Red represents the genes that were induced by the treatment ($Log_2FC < -1$) while green represents those that were repressed ($Log_2FC > 1$), Grey: $^{-}1 \geq Log_2\ FC \leq 1$.

3.3. Transcriptomic signatures reveal nano-specific effects

Transcriptomic effects were first inferred from the number of DEGs and the magnitude of their regulation. Conclusions that were based upon Venn diagrams (**Figure 2.B**) were further substantiated by PCA (**Figure A.8.B**). Indeed, 106 genes were differentially expressed in response to ionic Ce but not to the Ce ENPs (**Figure 2.A)**. Among those genes, 52 were differentially expressed with respect to both the control and the ENP ($Log_2FC > |1|$, $p_{adj} < 0.001$) (**Figure A.10.A)**. Of the 688 transcripts that were differentially expressed in response to the uncoated Ce ENPs, about one quarter (167 of the 688 DEGs, **Figure 2.B**) were also differentially expressed with respect to the exposure to ionic Ce ($Log_2FC > |1|$, $p_{adj} < 0.001$), *i.e.* most transcripts were specific to the uncoated Ce ENPs.

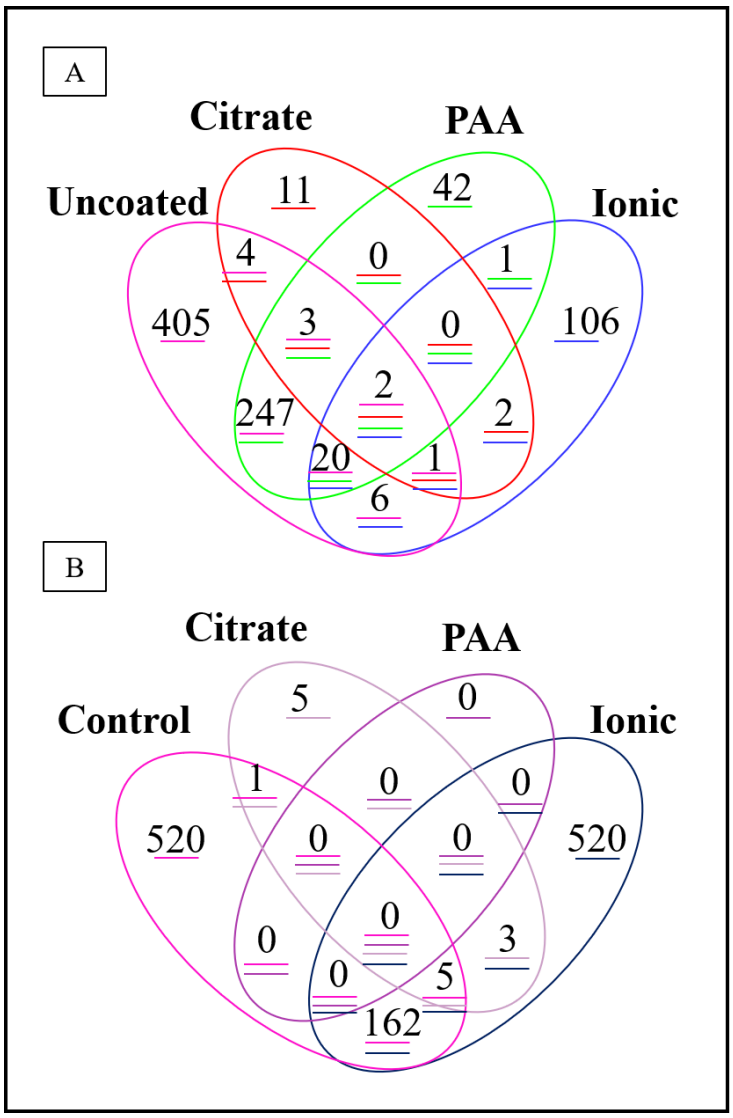

Figure 2. – (A) Differentially expressed genes with respect to the control ($Log_2FC > |1|$, $p_{adj} < 0.001$), following a 2 h exposure of *C. reinhardtii* to uncoated Ce ENPs (39.3 ± 10.0 µg L^{-1}), citrate stabilized Ce ENPs (33.2 ± 5.6 µg L^{-1}), PAA coated Ce ENPs (70.7 ± 2.2 µg L^{-1}), and ionic Ce (60.7 ± 3.9 µg L^{-1}). In (B), exposures were normalized to the uncoated Ce ENPs, rather than the control treatment ($Log_2FC > |1|$, $p_{adj} < 0.001$).

At the pathway level, our data were consistent with the Ce ENPs having a specific impact on cell motility and organization (**Table A.2, Figure A.9, and Supplementary Data 3**). For example, of the 26 transcripts linked to cellular flagella biogenesis and functioning and which were regulated by the Ce ENPs, 17 have been identified as being up-regulated during deflagellation in *C. reinhardtii,*[62] suggesting that this process plays a key role in the acclimation of microalgae to Ce ENPs. For instance, uncoated and PAA coated Ce ENPs induced the expression of *FAP16*, a gene involved in a pathway that induces detachment of the flagella[63] and both repressed the expression of a gene (*POC7*) related to flagella assembly.[64] Deflagellation could reduce physical exposure to ENPs via two mechanisms. First, as flagella are large structures surrounded by a bare plasma membrane, i.e. without a surrounding cell wall,[65] they may be more accessible to ENPs. Second, in *C. reinhardtii*, endocytosis is localized in a specialized region of the plasma membrane located at the base of the flagella.[66] Deflagellation might thus reduce Ce ENPs access to this region and, thereby, reduce biological membrane to interact with and/or cellular uptake by endocytosis.[67] If observed, deflagellation might suggest that *C. reinhardtii* are exposed to an unfavorable physicochemical environment (e.g. pH shock, heat, alcohol treatment).[65]

Transcript levels of genes involved in the xenobiotic resistance system increased when microalgae where exposed to the Ce ENPs unlike in cells exposed to ionic Ce (**Figure 3, Supplementary Data 4**). Regulation of protein metabolism targets was also different for ionic Ce in comparison to the ENPs **(Supplementary Data 5**). For example, genes with functions in intracellular protein targeting were enriched for ionic Ce, while protein folding enrichment was found for uncoated Ce ENPs (Wilcoxon test, $p < 0.05$) (**Table A.2, Figure**

4). Furthermore, approximately half of the DEGs related to protein metabolism elicited by the uncoated Ce ENPs had annotated functions in post-translational protein modification, a sub-pathway that was not identified to the same extent in cells exposed to ionic Ce (**Table A.2, Figure 4)**. Potential significance of this nano-effect is unclear because post-translational modifications occur in most metabolic pathways.

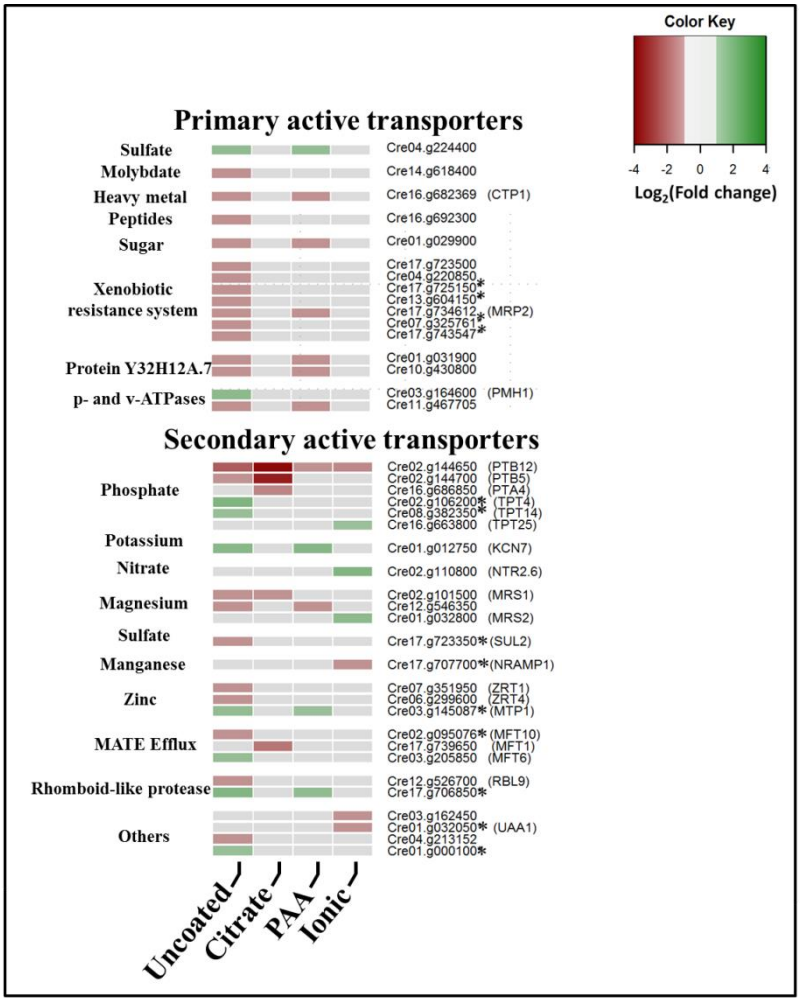

Figure 3. – Heat maps depicting fold changes in transcript levels of transport-related genes regulated by uncoated Ce ENPs (39.33 ± 10.02 µg L^{-1})), citrate stabilized Ce ENPs

(33.2 ± 5.6 µg L^{-1}), PAA coated Ce ENPs (70.7 ± 2.2 µg L^{-1}), and ionic Ce (60.7 ± 3.9 µg L^{-1}) with respect to control ($Log_2FC > |1|$, $p_{adj} < 0.001$) following a 2 h exposure of *C. reinhardtii*. Red represents the genes that were induced by the treatment ($Log_2FC < -1$) while green represents those that were repressed ($Log_2FC > 1$), Grey: $-1 \geq Log_2 FC \leq 1$. Acronyms are given for genes with annotated functions. Asterisks indicate genes that are differentially expressed between uncoated Ce ENPs and ionic Ce ($Log_2FC > |1|$, $p_{adj} < 0.001$).

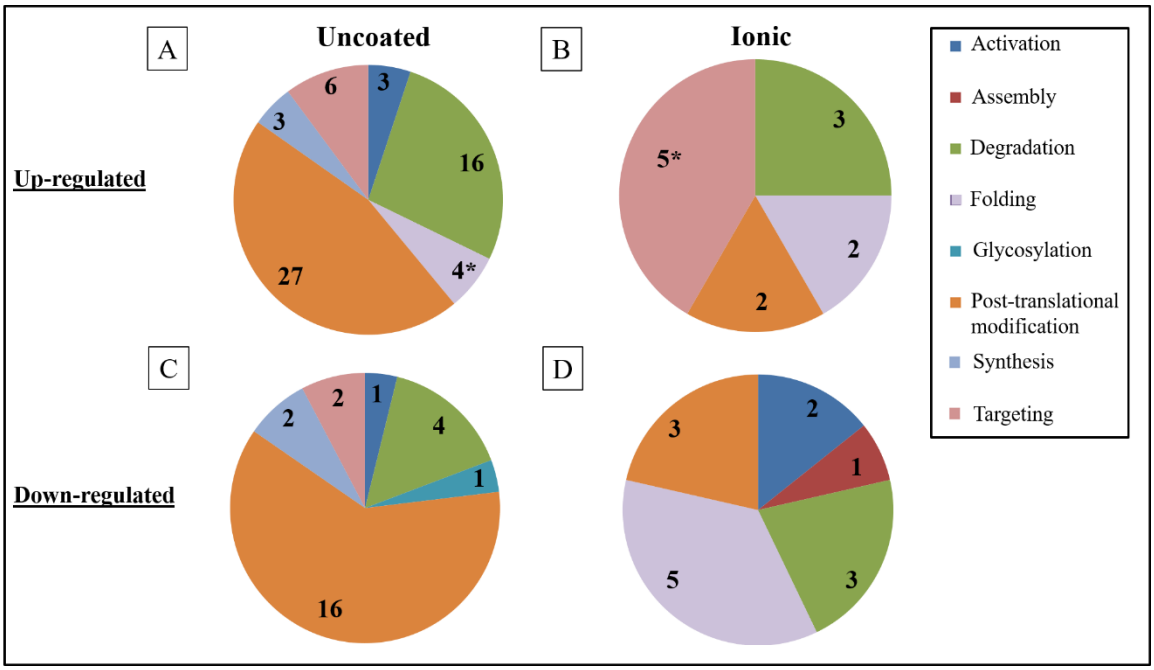

Figure 4. – Up-regulated (A, B) and down-regulated (C, D) gene percentages for different sub-pathways of protein metabolism in *C. reinhardtii* exposed to uncoated Ce ENPs (A, C) and ionic Ce (B, D). The numbers represent the number of DEGs (DeSeq2, $Log_2FC > |1|$, $p_{adj} < 0.001$). Asterisks indicate enriched molecular sub-pathways (Wilcoxon test, $p < 0.05$).

Combination of the above results strongly suggests that bioavailability was different for ionic and particulate forms of Ce. Although the above discussion focused largely on the uncoated Ce ENPs, very similar results were found for the PAA coated ENPs (discussed further below), in agreement with the PCA plot (**Figure A.8**). In contrast, exposure to the citrate stabilized Ce ENPs induced several pathways that were common with those induced following exposure to ionic Ce (e.g. no implication of the xenobiotic resistance system). Differences among the different ENPs are discussed in the following section.

3.4. RNA-Seq profiling revealed differences (and similarities) among the effects of Ce ENP coatings

As above, differences among the different ENP particle coatings were inferred from DEG numbers, the magnitude and direction of their regulation and pathways in which they are known to function (**Table A.2, Figure A.9**). For example, Ce ENPs with a citrate stabilized coating resulted in only 23 DEGs, whereas uncoated and PAA coated Ce ENPs induced 688 and 315 DEGs, respectively (**Figures 1 and 2**). The relatively weak transcriptomic response to the citrate stabilized Ce ENPs was consistent with observations performed on a cultured human cell line (72 h, 21.25 mg L^{-1}) where only 13 DEGs were detected after exposure to a similar citrate stabilized ENPs whereas 1643 DEGs were induced following exposure to small uncoated Ce ENPs (3 nm).[24]

The majority of DEGs elicited by a given Ce ENP were not elicited by any of the other Ce ENPs (**Figure 2A**). Nonetheless, some overlap of the signatures of two or all three of the Ce ENPs suggest the occurrence of common nano-effects. For example, transcriptomes of microalgae exposed to the uncoated Ce ENPs do not significantly differ

from those exposed to PAA coated ENPs ($Log_2FC > |1|$, $p_{adj} < 0.001$) (**Figure 2B, Figure A.10.C**) in spite of important differences in their physicochemical properties (i.e. Ce(III)/Ce(IV) ratio, surface coatings) and their resulting stabilities (i.e. agglomeration state) (**Table 1**). Moreover, 247 DEGs were common to the uncoated and PAA coated Ce ENPs, however, only 5 DEGs were common to the three Ce ENPs (**Figure 2A**). Of the 688 DEGs that were identified for the uncoated ENPs ($Log_2FC > |1|$, $p_{adj} < 0.001$), 6 were also differentially expressed with respect to citrate stabilized Ce ENPs ($Log_2FC > |1|$, $p_{adj} < 0.001$) (**Figure 2B**).

For each of the three Ce ENP types, ontological analysis (MapMan) was carried out to identify biological processes involving multiple DEGs **(Table A.2, Supplementary Data 2**). A major observation was that the uncoated and PAA coated altered expression of genes in protein metabolism (i.e. 85 DEGs for uncoated; 41 DEGs for PAA coated; **Table A.2, Figure A.9, Supplementary Data 5**). Such effect was not induced by citrate stabilized Ce ENPs. For example, uncoated and PAA coated Ce ENPs altered the expression of proteins involved in protein folding and selective protein degradation by the ubiquitin-proteasome system (UPS) (i.e. 13 DEGs for uncoated; 5 DEGs for PAA coated) (**Supplementary Data 5**). However, significant enrichment of protein folding was only found for uncoated Ce ENPs (Wilcoxon test, $p < 0.05$, **Figure 4, Table A.2**). In *C. reinhardtii,* increases in proteasome activity and protein ubiquitination have previously been reported to occur during various abiotic stresses,[68] e.g. exposure to selenite.[69] Another study found upregulation of transcripts encoding proteasome subunits during exposures to TiO_2 ENPs, ZnO ENPs or quantum dots.[44] As molecular chaperones and the UPS manage

non-native proteins, these results might reflect the propensity of these Ce ENPs to cause protein damage, misfolding, or both.

Another clear difference between the effects of the citrate stabilized Ce ENPs and the two other ENPs involved the active trans-membrane transport of small molecules (**Figure 3)**. These include the upregulation of transcripts encoding primary active transporters related to detoxification;[70,71] pleiotropic drug resistance proteins and P-glycoproteins and multidrug resistance associated proteins of the xenobiotic resistance system (**Supplementary Data 4**). Members of these protein families are also up-regulated following exposure to cadmium,[43] mercury[72] or aluminum.[73] Additionally, citrate stabilized Ce ENPs upregulated the expression of a secondary active transporter (*MFT1*) that may be involved with xenobiotic sequestration or efflux (**Figure 3**).[74] In rice, *MFT1* is induced by exposure to Al and is suspected to drive the efflux of Al-citrate.[75]

Phosphate and magnesium transporters were notable in that they were affected by all of the treatments, although phosphate transport enrichment was only found for the uncoated and citrate stabilized Ce ENPs (**Table A.2, Figure 3)**. As the secondary active transporters were up-regulated and each is selective for Mg[76] or phosphate[77] **(Supplementary Data 4)**, their induction likely reflected perturbations of both phosphate and magnesium homeostasis rather than Ce biouptake. For example, a type B high affinity phosphate transporter (*PTB12*) is thought to lead to increased internalization of phosphate,[77] and its strong induction found for all treatments likely reflects the ability of ionic Ce and Ce ENPs to reduce phosphate bioavailability either through direct competition for phosphate or after hydrolysis of phosphate ester bonds.[78] Similarly, two results strongly suggest that these responses do not reflect the induction of Ce *efflux*. First, there was no

effect on the expression of the candidate Ce transporters (e.g. non-specific metal transporter such as permeases[79] or Ca^{2+} channels[80]) by ionic Ce or the Ce ENPs, (**Supplementary Data 4**). Second, for cells exposed to ionic Ce, no regulation of transcription was observed for genes involved in the xenobiotic resistance system, in contrast to results for the ENPs.

3.5. Ce and Ce ENPs induce genes for acclimation, but not major cellular damage

None of the Ce forms (ionic or ENPs) appeared to be particularly toxic to *C. reinhardtii* at 70 µg L^{-1} Ce (nominal concentration). For example, no damage biomarkers (e.g. DNA damage or apoptosis signaling) were induced by any of the Ce treatments. Furthermore, the up-regulation of key oxidative stress enzymes involved in the detoxification of reactive oxygen species (e.g. catalase acting in peroxisomes[81]) was not observed (**Supplementary Data 6**). The absence of clear evidence for toxicity is reasonable, considering the sub-lethal exposure concentrations and the short exposure times that were used. Indeed, with the notable exception of a 72h EC50 value for growth inhibition that was 26 µg L^{-1} for PAA coated Ce ENPs[12], much higher (i.e. mg L^{-1}) concentrations of Ce ENPs are generally required to induce toxicity (e.g. lowest-observed-effect concentration (LOEC) of >1 mg L^{-1} for a 72 h exposure of *P. subcapitata*[82]). However, transcript levels of genes related to flagella structure were specifically impacted by Ce ENPs. The uncoated and the PAA coated Ce ENPs also up-regulated mRNA levels of biomarkers of detoxification processes. The molecular responses observed for our exposure conditions (2h, <70 µg L^{-1}), are thus thought to mainly reflect biological responses that allow the microalgae to manage stress.

4. Conclusions and perspectives

The experiment was designed to compare the transcriptional effects of three ENPs and to establish their relative biological availability to *C. reinhardtii*. Nominally, the three ENPs had similar sizes, compositions and concentrations. In reality, careful characterization showed that: (i) uncoated Ce ENPs agglomerated significantly; (ii) citrate stabilized Ce ENPs showed limited agglomeration; (iii) some or a majority of the Ce(IV) in the PAA stabilized Ce ENPs was transformed into Ce(III) (either adsorbed Ce^{3+} or Ce_2O_3); (iv) dissolved solutions of ionic Ce actually contained significant quantities of Ce nanoparticles (likely metastable Ce polymers due to hydrolysis). Thus, extensive characterization is necessary in order to properly interpret complex, high throughput exposures examining the biological effects of engineered nanomaterials. While this point may seem obvious to most, some reports characterize only the stock solutions. Our multi-method characterization showed that different results were obtained for the concentrations and experimental conditions used for the exposures.

The transcriptomic results revealed that (i) the Ce ENPs examined in this study are bioavailable; (ii) Ce ENPs had nano-effects that were distinct from the effects of ionic Ce; (iii) coatings could affect the bioavailability and biological effects of Ce ENPs. In spite of their different sizes, surface charge/coating and Ce(III)/Ce(IV) ratios, uncoated and PAA coated Ce ENPs exhibited few differences with respect to the molecular targets examined at transcriptomic level. One potential explanation is that after microalgae introduction, protein corona or microalgal exudates homogenizes the different ENPs, at least in relation to the microorganism at the level of the biological interface. This also implies that it was the citrate released from the citrate stabilized ENPs that was responsible for the fewest

effects on the microalgae observed for that particle. Free citrate in solution could either complex Ce, reducing its bioavailability, or stimulate the microalgae as a fundamental metabolite.

C. reinhardtii appeared to acclimate to Ce ENPs by remodeling of the UPS, moderate increases in the expression of molecular chaperones and by alterations of the flagella or deflagellation that might reflect a middle stress for short term exposures at environmentally relevant concentrations. However, biological interpretations of the transcriptomic results were limited by the quantity and quality of gene annotation available for *C. reinhardtii* as well as the lack of integrative tools required to interpret the data. For example, important numbers of genes responding to Ce ENPs and/or ionic Ce were either not assigned to a biological pathway (i.e. 244 DEGs) or not associated with a known function (i.e. 266 DEGs) (**Supplementary Data 7**). Thus, it is possible that some key deleterious or beneficial responses might have not been explored completely in the present study.

A promising pool of Ce-responsive genes was identified, which may constitute interesting exposure biomarkers for future experiments and bioassay development (**Supplementary Data 8)**. For example, g15615, a putative ferredoxin was repressed by ionic Ce but induced by uncoated Ce ENPs. Although whole-genome expression analysis provided important information on the potential biological effects of the Ce ENPs, different exposure times, exposure concentrations and biological scales (proteomic and metabolomics) will be required in order to provide more complete information on the impact of the Ce ENPs at the scale of the organism or population. Indeed, important post-transcriptional modifications that have not been considered here may occur in *C.*

reinhardtii. Furthermore, for different exposure durations or concentration scales, other management strategies may be put into play, resulting in the activation of other important genes and metabolic pathways.

.

ACKNOWLEDGEMENTS

Special thanks to Madjid Hadioui (University of Montreal) for his expert advice on the ICP-MS and SP-ICP-MS analyses and to Yanxia Wu (Concordia University) for sharing her expertise with the RNA extraction of *C. reinhardtii*.

FUNDING

Funding for this work was provided by the Natural Sciences and Engineering Research Council of Canada (NSERC Discovery and Strategic projects grants) and the Fonds de Recherche du Québec - Nature et Technologies (FRQNT). Special thanks to Madjid Hadioui for his expert advice on the ICP-MS and SP-ICP-MS analyses.

CONFLICTS OF INTEREST

There are no conflicts of interest to declare.

REFERENCES

1. Goodenough, K. M.; Wall, F.; Merriman, D. J. N. R. R., The rare earth elements: demand, global resources, and challenges for resourcing future generations. **2018,** *27*, (2), 201-216.

2. Moss, R.; Tzimas, E.; Willis, P.; Arendorf, J.; Thompson, P.; Chapman, A.; Morley, N.; Sims, E.; Bryson, R.; Peason, J. *Critical metals in the path towards the decarbonisation of the EU energy sector*; EUR 25994 EN European commission 2013, **2013**.

3. Reed, K.; Cormack, A.; Kulkarni, A.; Mayton, M.; Sayle, D.; Klaessig, F.; Stadler, B., Exploring the properties and applications of nanoceria: is there still plenty of room at the bottom? *Environmental Science: Nano* **2014,** *1*, (5), 390-405.

4. Pramanik, B. K.; Nghiem, L. D.; Hai, F. I. J. W. r., Extraction of strategically important elements from brines: Constraints and opportunities. **2020,** *168*, 115149.

5. Loddo, V.; Yurdakal, S.; Parrino, F., Economical aspects, toxicity, and environmental fate of cerium oxide. In *Cerium Oxide (CeO_2): Synthesis, Properties and Applications*, Elsevier: 2020; pp 359-373.

6. Cassee, F. R.; van Balen, E. C.; Singh, C.; Green, D.; Muijser, H.; Weinstein, J.; Dreher, K., Exposure, health and ecological effects review of engineered nanoscale cerium and cerium oxide associated with its use as a fuel additive. *Critical Reviews in Toxicology* **2011,** *41*, (3), 213-229.

7. Johnson, A. C.; Park, B., Predicting contamination by the fuel additive cerium oxide engineered nanoparticles within the United Kingdom and the associated risks. *Environmental Toxicology and Chemistry* **2012,** *31*, (11), 2582-2587.

8. Giese, B.; Klaessig, F.; Park, B.; Kaegi, R.; Steinfeldt, M.; Wigger, H.; von Gleich, A.; Gottschalk, F. J. S. r., Risks, release and concentrations of engineered nanomaterial in the environment. **2018,** *8*, (1), 1-18.

9. Walkey, C.; Das, S.; Seal, S.; Erlichman, J.; Heckman, K.; Ghibelli, L.; Traversa, E.; McGinnis, J. F.; Self, W. T., Catalytic properties and biomedical applications of cerium oxide nanoparticles. *Environmental Science: Nano* **2015,** *2*, (1), 33-53.

10. White, J. C.; Gardea-Torresdey, J., Achieving food security through the very small. *Nature Nanotechnology* **2018,** *13*, (8), 627.

11. Feng, Y.; Lu, H.; Liu, Y.; Xue, L.; Dionysiou, D. D.; Yang, L.; Xing, B., Nano-cerium oxide functionalized biochar for phosphate retention: preparation, optimization and rice paddy application. *Chemosphere* **2017,** *185*, 816-825.

12. Booth, A.; Størseth, T.; Altin, D.; Fornara, A.; Ahniyaz, A.; Jungnickel, H.; Laux, P.; Luch, A.; Sørensen, L., Freshwater dispersion stability of PAA-stabilised cerium oxide nanoparticles and toxicity towards Pseudokirchneriella subcapitata. *Science of the Total Environment* **2015,** *505*, 596-605.

13. Taylor, N. S.; Merrifield, R.; Williams, T. D.; Chipman, J. K.; Lead, J. R.; Viant, M. R., Molecular toxicity of cerium oxide nanoparticles to the freshwater alga

Chlamydomonas reinhardtii is associated with supra-environmental exposure concentrations. *Nanotoxicology* **2016,** *10*, (1), 32-41.

14. Hoecke, K. V.; Quik, J. T.; Mankiewicz-Boczek, J.; Schamphelaere, K. A. D.; Elsaesser, A.; Meeren, P. V. d.; Barnes, C.; McKerr, G.; Howard, C. V.; Meent, D. V. D., Fate and effects of CeO2 nanoparticles in aquatic ecotoxicity tests. *Environmental Science & Technology* **2009,** *43*, (12), 4537-4546.

15. Röhder, L. A.; Brandt, T.; Sigg, L.; Behra, R., Influence of agglomeration of cerium oxide nanoparticles and speciation of cerium (III) on short term effects to the green algae Chlamydomonas reinhardtii. *Aquatic Toxicology* **2014,** *152*, 121-130.

16. Dhall, A.; Self, W., Cerium oxide nanoparticles: a brief review of their synthesis methods and biomedical applications. *Antioxidants* **2018,** *7*, (8), 97.

17. Sendra, M.; Yeste, P.; Moreno-Garrido, I.; Gatica, J.; Blasco, J., CeO2 NPs, toxic or protective to phytoplankton? Charge of nanoparticles and cell wall as factors which cause changes in cell complexity. *Science of The Total Environment* **2017,** *590*, 304-315.

18. Navarro, E.; Baun, A.; Behra, R.; Hartmann, N. B.; Filser, J.; Miao, A.-J.; Quigg, A.; Santschi, P. H.; Sigg, L., Environmental behavior and ecotoxicity of engineered nanoparticles to algae, plants, and fungi. *Ecotoxicology* **2008,** *17*, (5), 372-386.

19. Auffan, M.; Masion, A.; Labille, J.; Diot, M.-A.; Liu, W.; Olivi, L.; Proux, O.; Ziarelli, F.; Chaurand, P.; Geantet, C., Long-term aging of a CeO2 based nanocomposite used for wood protection. *Environmental Pollution* **2014,** *188*, 1-7.

20. Barton, L. E.; Auffan, M.; Bertrand, M.; Barakat, M.; Santaella, C.; Masion, A.; Borschneck, D.; Olivi, L.; Roche, N.; Wiesner, M. R., Transformation of pristine and citrate-functionalized CeO2 nanoparticles in a laboratory-scale activated sludge reactor. *Environmental Science & Technology* **2014,** *48*, (13), 7289-7296.

21. Andreescu, D.; Bulbul, G.; Özel, R. E.; Hayat, A.; Sardesai, N.; Andreescu, S., Applications and implications of nanoceria reactivity: measurement tools and environmental impact. *Environmental Science: Nano* **2014,** *1*, (5), 445-458.

22. Pulido-Reyes, G.; Rodea-Palomares, I.; Das, S.; Sakthivel, T. S.; Leganes, F.; Rosal, R.; Seal, S.; Fernández-Piñas, F., Untangling the biological effects of cerium oxide nanoparticles: the role of surface valence states. *Scientific Reports* **2015,** *5*, 15613.

23. Asati, A.; Santra, S.; Kaittanis, C.; Perez, J. M., Surface-charge-dependent cell localization and cytotoxicity of cerium oxide nanoparticles. *ACS Nano* **2010,** *4*, (9), 5321-5331.

24. Fisichella, M.; Berenguer, F.; Steinmetz, G.; Auffan, M.; Rose, J.; Prat, O., Toxicity evaluation of manufactured CeO 2 nanoparticles before and after alteration: combined physicochemical and whole-genome expression analysis in Caco-2 cells. *BMC Genomics* **2014,** *15*, (1), 700.

25. Hussain, S. M.; Warheit, D. B.; Ng, S. P.; Comfort, K. K.; Grabinski, C. M.; Braydich-Stolle, L. K., At the crossroads of nanotoxicology in vitro: past achievements and current challenges. *Toxicological Sciences* **2015,** *147*, (1), 5-16.

26. Manier, N.; Bado-Nilles, A.; Delalain, P.; Aguerre-Chariol, O.; Pandard, P., Ecotoxicity of non-aged and aged CeO2 nanomaterials towards freshwater microalgae. *Environmental Pollution* **2013,** *180*, 63-70.

27. Rodea-Palomares, I.; Boltes, K.; Fernández-Pinas, F.; Leganés, F.; García-Calvo, E.; Santiago, J.; Rosal, R., Physicochemical characterization and ecotoxicological assessment of CeO2 nanoparticles using two aquatic microorganisms. *Toxicological Sciences* **2010,** *119*, (1), 135-145.

28. Rogers, N. J.; Franklin, N. M.; Apte, S. C.; Batley, G. E.; Angel, B. M.; Lead, J. R.; Baalousha, M., Physico-chemical behaviour and algal toxicity of nanoparticulate CeO2 in freshwater. *Environmental Chemistry* **2010,** *7*, (1), 50-60.

29. Keller, A. A.; Lazareva, A., Predicted releases of engineered nanomaterials: from global to regional to local. *Environmental Science & Technology Letters* **2013,** *1*, (1), 65-70.

30. Klaper, R.; Arndt, D.; Bozich, J.; Dominguez, G., Molecular interactions of nanomaterials and organisms: defining biomarkers for toxicity and high-throughput screening using traditional and next-generation sequencing approaches. *Analyst* **2014,** *139*, (5), 882-895.

31. Ruotolo, R.; Maestri, E.; Pagano, L.; Marmiroli, M.; White, J. C.; Marmiroli, N., Plant response to metal-containing engineered nanomaterials: an omics-based perspective. *Environmental Science & Technology* **2018,** *52*, (5), 2451-2467.

32. Lee, T.-L.; Raitano, J. M.; Rennert, O. M.; Chan, S.-W.; Chan, W.-Y., Accessing the genomic effects of naked nanoceria in murine neuronal cells. *Nanomedicine: Nanotechnology, Biology and Medicine* **2012,** *8*, (5), 599-608.

33. Abràmoff, M. D.; Magalhães, P. J.; Ram, S. J., Image processing with ImageJ. *Biophotonics International* **2004,** *11*, (7), 36-42.

34. Collins, T. J., ImageJ for microscopy. *Biotechniques* **2007,** *43*, (S1), S25-S30.

35. Frechette-Viens, L.; Hadioui, M.; Wilkinson, K. J., Quantification of ZnO Nanoparticles and other Zn Containing Colloids in Natural Waters Using a High Sensitivity Single Particle ICP-MS. *Talanta (In press)* **2019**.

36. Shaw, P.; Donard, A., Nano-particle analysis using dwell times between 10 μs and 70 μs with an upper counting limit of greater than 3× 10 7 cps and a gold nanoparticle detection limit of less than 10 nm diameter. *Journal of Analytical Atomic Spectrometry* **2016,** *31*, (6), 1234-1242.

37. Newman, K.; Metcalfe, C.; Martin, J.; Hintelmann, H.; Shaw, P.; Donard, A., Improved single particle ICP-MS characterization of silver nanoparticles at environmentally relevant concentrations. *Journal of Analytical Atomic Spectrometry* **2016,** *31*, (10), 2069-2077.

38. Diaz, L.; Peyrot, C.; Wilkinson, K. J., Characterization of Polymeric Nanomaterials Using Analytical Ultracentrifugation. *Environmental Science & Technology* **2015,** *49*, (12), 7302-7309.

39. Harris, E., Culture and storage methods. *The Chlamydomonas Sourcebook. A Comprehensibe Guide to Biology and Laboratory Use* **1989**, 25-63.

40. Kola, H.; Wilkinson, K. J., Cadmium uptake by a green alga can be predicted by equilibrium modelling. *Environmental Science & Technology* **2005,** *39*, (9), 3040-3047.

41. Kola, H.; Laglera, L. M.; Parthasarathy, N.; Wilkinson, K. J., Cadmium adsorption by Chlamydomonas reinhardtii and its interaction with the cell wall proteins. *Environmental Chemistry* **2004,** *1*, (3), 172-179.

42. Azimzada, A.; Tufenkji, N.; Wilkinson, K. J., Transformations of silver nanoparticles in wastewater effluents: links to Ag bioavailability. *Environmental Science: Nano* **2017,** *4*, (6), 1339-1349.

43. Simon, D. F.; Descombes, P.; Zerges, W.; Wilkinson, K. J., Global expression profiling of Chlamydomonas reinhardtii exposed to trace levels of free cadmium. *Environmental Toxicology and Chemistry* **2008,** *27*, (8), 1668-1675.

44. Simon, D. F.; Domingos, R. F.; Hauser, C.; Hutchins, C. M.; Zerges, W.; Wilkinson, K. J., RNA-Seq analysis of the effects of metal nanoparticle exposure on the transcriptome of Chlamydomonas reinhardtii. *Applied and Environmental Microbiology* **2013**, AEM. 00998-13.

45. Andrews, S., FastQC: a quality control tool for high throughput sequence data. Babraham Bioinformatics. *Online [Mar 2016]* **2010**.

46. Krueger, F., Trim galore. *A wrapper tool around Cutadapt and FastQC to consistently apply quality and adapter trimming to FastQ files* **2015**.

47. Kim, D.; Pertea, G.; Trapnell, C.; Pimentel, H.; Kelley, R.; Salzberg, S. L., TopHat2: accurate alignment of transcriptomes in the presence of insertions, deletions and gene fusions. *Genome Biology* **2013,** *14*, (4), R36.

48. Wang, L.; Wang, S.; Li, W., RSeQC: quality control of RNA-seq experiments. *Bioinformatics* **2012,** *28*, (16), 2184-2185.

49. Anders, S.; Pyl, P. T.; Huber, W., HTSeq—a Python framework to work with high-throughput sequencing data. *Bioinformatics* **2015,** *31*, (2), 166-169.

50. Love, M. I.; Huber, W.; Anders, S., Moderated estimation of fold change and dispersion for RNA-seq data with DESeq2. *Genome Biology* **2014,** *15*, (12), 550.

51. Usadel, B.; Poree, F.; Nagel, A.; Lohse, M.; CZEDIK-EYSENBERG, A.; Stitt, M., A guide to using MapMan to visualize and compare Omics data in plants: a case study in the crop species, Maize. *Plant, Cell & Environment* **2009,** *32*, (9), 1211-1229.

52. Thimm, O.; Bläsing, O.; Gibon, Y.; Nagel, A.; Meyer, S.; Krüger, P.; Selbig, J.; Müller, L. A.; Rhee, S. Y.; Stitt, M., MAPMAN: a user-driven tool to display genomics data sets onto diagrams of metabolic pathways and other biological processes. *The Plant Journal* **2004,** *37*, (6), 914-939.

53. Goodstein, D. M.; Shu, S.; Howson, R.; Neupane, R.; Hayes, R. D.; Fazo, J.; Mitros, T.; Dirks, W.; Hellsten, U.; Putnam, N., Phytozome: a comparative platform for green plant genomics. *Nucleic Acids Research* **2011,** *40*, (D1), D1178-D1186.

54. Lopez, D.; Casero, D.; Cokus, S. J.; Merchant, S. S.; Pellegrini, M., Algal Functional Annotation Tool: a web-based analysis suite to functionally interpret large gene lists using integrated annotation and expression data. *BMC Bioinformatics* **2011,** *12*, (1), 282.

55. Tella, M.; Auffan, M.; Brousset, L.; Morel, E.; Proux, O.; Chanéac, C.; Angeletti, B.; Pailles, C.; Artells, E.; Santaella, C., Chronic dosing of a simulated pond ecosystem in indoor aquatic mesocosms: fate and transport of CeO 2 nanoparticles. *Environmental Science: Nano* **2015,** *2*, (6), 653-663.

56. Tsunekawa, S.; Sivamohan, R.; Ito, S.; Kasuya, A.; Fukuda, T., Structural study on monosize CeO2-x nano-particles. *Nanostructured Materials* **1999,** *11*, (1), 141-147.

57. Tsunekawa, S.; Fukuda, T.; Kasuya, A., X-ray photoelectron spectroscopy of monodisperse CeO2− x nanoparticles. *Surface Science* **2000,** *457*, (3), L437-L440.

58. Zhang, F.; Wang, P.; Koberstein, J.; Khalid, S.; Chan, S.-W. J. S. S., Cerium oxidation state in ceria nanoparticles studied with X-ray photoelectron spectroscopy and absorption near edge spectroscopy. **2004,** *563*, (1-3), 74-82.

59. El-Akl, P.; Smith, S.; Wilkinson, K. J., Linking the chemical speciation of cerium to its bioavailability in water for a freshwater alga. *Environmental Toxicology and Chemistry* **2015,** *34*, (8), 1711-1719.

60. Grulke, E.; Reed, K.; Beck, M.; Huang, X.; Cormack, A.; Seal, S., Nanoceria: factors affecting its pro-and anti-oxidant properties. *Environmental Science: Nano* **2014,** *1*, (5), 429-444.

61. Blaby, I. K.; Blaby-Haas, C. E.; Tourasse, N.; Hom, E. F.; Lopez, D.; Aksoy, M.; Grossman, A.; Umen, J.; Dutcher, S.; Porter, M., The Chlamydomonas genome project: a decade on. *Trends in Plant Science* **2014,** *19*, (10), 672-680.

62. Zones, J. M.; Blaby, I. K.; Merchant, S. S.; Umen, J. G., High-resolution profiling of a synchronized diurnal transcriptome from Chlamydomonas reinhardtii reveals continuous cell and metabolic differentiation. *The Plant Cell* **2015,** *27*, (10), 2743-2769.

63. Hilton, L. K.; Meili, F.; Buckoll, P. D.; Rodriguez-Pike, J. C.; Choutka, C. P.; Kirschner, J. A.; Warner, F.; Lethan, M.; Garces, F. A.; Qi, J., A forward genetic screen and whole genome sequencing identify deflagellation defective mutants in Chlamydomonas, including assignment of ADF1 as a TRP channel. *G3: Genes, Genomes, Genetics* **2016**, g3. 116.034264.

64. Keller, L. C.; Romijn, E. P.; Zamora, I.; Yates III, J. R.; Marshall, W. F., Proteomic analysis of isolated chlamydomonas centrioles reveals orthologs of ciliary-disease genes. *Current Biology* **2005,** *15*, (12), 1090-1098.

65. Quarmby, L. M., Deflagellation. In *The Chlamydomonas Sourcebook*, Elsevier: 2009; pp 43-69.

66. Molla-Herman, A.; Ghossoub, R.; Blisnick, T.; Meunier, A.; Serres, C.; Silbermann, F.; Emmerson, C.; Romeo, K.; Bourdoncle, P.; Schmitt, A., The ciliary pocket: an endocytic membrane domain at the base of primary and motile cilia. *J Cell Sci* **2010,** *123*, (10), 1785-1795.

67. Pulido-Reyes, G.; Briffa, S. M.; Hurtado-Gallego, J.; Yudina, T.; Leganés, F.; Puntes, V.; Valsami-Jones, E.; Rosal, R.; Fernández-Piñas, F., Internalization and toxicological mechanisms of uncoated and PVP-coated cerium oxide nanoparticles in the freshwater alga Chlamydomonas reinhardtii. *Environmental Science: Nano* **2019,** *6*, (6), 1959-1972.

68. Lyzenga, W. J.; Stone, S. L., Abiotic stress tolerance mediated by protein ubiquitination. *Journal of Experimental Botany* **2011,** *63*, (2), 599-616.

69. Vallentine, P.; Hung, C.-Y.; Xie, J.; Van Hoewyk, D., The ubiquitin–proteasome pathway protects Chlamydomonas reinhardtii against selenite toxicity, but is impaired as reactive oxygen species accumulate. *AoB Plants* **2014,** *6*.

70. Lane, T. S.; Rempe, C. S.; Davitt, J.; Staton, M. E.; Peng, Y.; Soltis, D. E.; Melkonian, M.; Deyholos, M.; Leebens-Mack, J. H.; Chase, M., Diversity of ABC transporter genes across the plant kingdom and their potential utility in biotechnology. *BMC Biotechnology* **2016,** *16*, (1), 47.

71. Schulz, B.; Kolukisaoglu, H. Ü., Genomics of plant ABC transporters: the alphabet of photosynthetic life forms or just holes in membranes? *FEBS Letters* **2006,** *580*, (4), 1010-1016.

72. Beauvais-Flück, R.; Slaveykova, V. I.; Cosio, C., Cellular toxicity pathways of inorganic and methyl mercury in the green microalga Chlamydomonas reinhardtii. *Scientific Reports* **2017,** *7*, (1), 8034.

73. Yokosho, K.; Yamaji, N.; Ma, J. F., Global transcriptome analysis of Al-induced genes in an Al-accumulating species, common buckwheat (Fagopyrum esculentum Moench). *Plant and Cell Physiology* **2014,** *55*, (12), 2077-2091.

74. Takanashi, K.; Shitan, N.; Yazaki, K., The multidrug and toxic compound extrusion (MATE) family in plants. *Plant Biotechnology* **2014,** *31*, (5), 417-430.

75. Yokosho, K.; Yamaji, N.; Ma, J. F., An Al-inducible MATE gene is involved in external detoxification of Al in rice. *The Plant Journal* **2011,** *68*, (6), 1061-1069.

76. Li, L.; Tutone, A. F.; Drummond, R. S.; Gardner, R. C.; Luan, S., A novel family of magnesium transport genes in Arabidopsis. *The Plant Cell* **2001,** *13*, (12), 2761-2775.

77. Moseley, J.; Grossman, A. R., Phosphate metabolism and responses to phosphorus deficiency. In *The Chlamydomonas Sourcebook*, Elsevier: 2009; pp 189-215.

78. Kuchma, M. H.; Komanski, C. B.; Colon, J.; Teblum, A.; Masunov, A. E.; Alvarado, B.; Babu, S.; Seal, S.; Summy, J.; Baker, C. H., Phosphate ester hydrolysis of biologically relevant molecules by cerium oxide nanoparticles. *Nanomedicine: Nanotechnology, Biology and Medicine* **2010,** *6*, (6), 738-744.

79. Blaby-Haas, C. E.; Merchant, S. S., The ins and outs of algal metal transport. *Biochimica et Biophysica Acta (BBA)-Molecular Cell Research* **2012,** *1823*, (9), 1531-1552.

80. Perullini, M.; Bilmes, S. A. A.; Jobbágy, M., Cerium oxide nanoparticles: structure, applications, reactivity, and eco-toxicology. In *Nanomaterials: A Danger or a Promise?*, Springer: 2013; pp 307-333.

81. Mittler, R., Oxidative stress, antioxidants and stress tolerance. *Trends in Plant Science* **2002,** *7*, (9), 405-410.

82. Collin, B.; Auffan, M.; Johnson, A. C.; Kaur, I.; Keller, A. A.; Lazareva, A.; Lead, J. R.; Ma, X.; Merrifield, R. C.; Svendsen, C., Environmental release, fate and ecotoxicological effects of manufactured ceria nanomaterials. *Environmental Science: Nano* **2014,** *1*, (6), 533-548.